Theoret. Chim. Acta (Berl.) 39, 149—160 (1975)

Theoretical Study of the H_5^+ System

Reinhart Ahlrichs

Institut für Physikalische Chemie und Elektrochemie der Universität Karlsruhe, Germany

Received March 11, 1975

Ab initio calculations have been carried out for the ground state of H_5^+ in order to predict its equilibrium geometry, binding energy, enthalpy of formation, and the features of the $H_2 \cdot H_3^+$ interaction at large and intermediate intermolecular distances. The extended basis set of Gaussian functions was carefully optimized to describe the various kinds of intermolecular interactions. Electron correlation was accounted for by means of CI calculations. Different from previous studies we find a D_{2d} equilibrium geometry with $D_e = 7.4$ kcal/mol and $\Delta H^0_{300} \approx -8.7$ kcal/mol. The potential surface turns out to be extremely shallow in the vicinity of the D_{2d} structure which results in a great mobility of the central nucleus at room temperature.

Key words: H_5^+, geometry and stability of $\sim$ – correlation in H_5^+

1. Introduction

Although experimental [1–7] and theoretical [8–12] investigations clearly prove the stability of H_5^+ (with respect to any kind of dissociation) little is known about properties of this molecule. From experiments one has obtained estimates for ΔH^0 of the reaction (1)

$$H_2 + H_3^+ = H_5^+ \,. \tag{1}$$

Two recent experimental values for ΔH^0 are

$$\Delta H^0 = -5.1 \pm 0.6 \text{ kcal/mol [6]}$$

$$\Delta H^0 = -9.7 \pm 0.2 \text{ kcal/mol [7]}\,.$$

Various studies have been proformed to determine the equilibrium geometry [8–12] and vibrational frequences [8, 12] of H_5^+ by means of quantum mechanical computations. As a main result of these studies it turns out that H_5^+ is far from being a rigid molecule [12]. For this reason it has proved difficult to predict even the geometry of H_5^+. Whereas some earlier treatments predicted a D_{2d} structure [8, 9] the most recent and most accurate computations indicate that H_5^+ forms an ion cluster $H_3^+ \cdot H_2$, held together mainly by ion-induced dipole attraction [11, 12].

In order to obtain an accurate description of this interaction it is necessary to use specially adapted and extended basis sets [13, 14]. The so far most accurate treatment of H_5^+ has been published by Salmon and Poshusta [12] who allowed for a polarization of the Hydrogen AO's and thus included explicitly the ion

induced dipole interaction. Due to the special form of the wavefunction used by these authors it is rather difficult to assess the flexibility of their trial function. The total energy reported by Salmon and Poshusta was estimated by these authors to be about 0.04 a.u. above the exact one.

The present computations were performed with a method that goes beyond the HF approximation and includes effects of electron correlation like dispersion interaction and intramolecular correlation.

The basis set was carefully optimized to account for all relevant types of intermolecular interactions like ion-quadrupole-, ion- induced-dipole- and dispersion interaction and also changes in intramolecular correlation energies. Our computed total electronic energies are about 0.01 a.u. above the estimated exact energies. Due to the careful choice of this basis set we expect the relative errors to be almost an order of magnitude smaller.

The main reason to start the present study were the results of recent molecular beam experiments performed by Ludwig and Teloy [15]. Preliminary measurements of the total cross section for the reactive scattering

$$H_2 + D_3^+ \rightarrow H_2D^+ + D_2\,, \tag{2}$$

$$H_2 + D_3^+ \rightarrow HD + D_2H^+\,, \tag{3}$$

showed that process (3) is favoured by roughly a factor of 2 (as compared to 2) at collision energies smaller than 0.1 eV, while process (2) predominates by far at energies higher than 0.2 eV.

Reaction 2 is a simple transfer of a nucleus from D_3^+ to H_2 which can proceed via a trasition state with D_{2d} or D_{2h} symmetry.

Reaction 3 may be understood as an exchange of two nuclei. If this process would proceed directly in a single step one would expect a barrier (like for the process $H_2 + D_2 \rightarrow 2\,HD$) which is in contradiction to the experimental results. Possible transition states for a single step mechanism (in which the opening and formation of the bonds to be changed proceeds simultaneously) may have a structure with T_d, C_{4v} or D_{5h} symmetry which all have an open shell 4-electron ground state expected to be higher in energy than $H_2 + H_3^+$.

Although the transition state may have a lower symmetry (than those just mentioned), the above reasoning still is basically correct for all the reaction paths we could think of for a single step mechanism. The ratio of the total cross sections for the channels (2) and (3), however, corresponds roughly to the statistical weight of the reaction products. This indicates that decay takes place after rather complete isomerization of a long lived H_5^+-complex. We have therefore especially investigated if the required isomerization is possible without additional activation energy.

2. Method of Computations

We start with a conventional closed shell Hartree-Fock (HF) computation. The correlation energy is then obtained by means of a PNO-CI (PNO = pseudo natural orbital [16] or pair natural orbital [17, 18], CI = configuration interaction) and CEPA [19, 18] (coupled electron pair approximation). The PNO-CI includes the doubly excited configurations in addition to the HF wave function and is

based on the PNO's of the respective pair functions [17]. The CEPA accounts also for the effect of higher than doubly substituted configurations although in an approximate way [19, 18]. The CEPA is consequently not a strictly variational method whereas the PNO-CI always yield an upper bound to the electronic energy.

Although the present author in general prefers the CEPA especiallly for the computation of reaction energies, see the discussion in reference [20, 21], there is little difference between the PNO-CI and CEPA results as far as energy differences for the various conformations of H_5^+ is concerned.

For the subsequent discussions it is convenient to decompose the total correlation energy into intra- (ε_{ii}) and interpair (ε_{ij}) contributions, for the present case of two HF-MO's:

$$\varepsilon = \varepsilon_{11} + \varepsilon_{22} + \varepsilon_{12} \,. \tag{4}$$

The decomposition (4) can be made for the PNO-CI as well as for the CEPA correlation energies [18, 19]. It depends, however, on the choice for the HF-MO's. In the present study we always use the Boys localized rather than the canonical MO's.

3. Basis Set and Accuracy

The basis set consisted of contracted Gaussian lobe functions described in Table 1. The *s* basis is a Huzinaga 6*s* set contracted (4, 1, 1).

The orbital exponents of the two *p* sets were determinand in the following way. The more spread out function ($\eta = 0.15$) is necessary to get an accurate result for the polarizability $\alpha_\perp$ of H_2. The steeper fuction ($\eta = 0.85$) was then chosen to optimize the total energy of H_2 at the equilibrium distance d (H–H) = 1.4 a.u.

Let us now discuss briefly the various kinds of intermolecular interactions between H_2 and H_3^+ in order to get an idea of the accuracly of HF and correlation energy computations with the present basis set.

The dominant long range interactions are, in an obvious notation, (H_3^+) monopole-(H_2) quadrupole interaction E_3 (R denotes the distance between the

Table 1. Gaussian AO basis for H_5^+

Type[a]	η	c[b]
s	68.160	0.007386
	10.2465	0.056140
	2.34648	0.268822
	0.67332	0.752376
s	0.22466	1.0
s	0.08222	1.0
p	0.85	1.0
p	0.15	1.0

[a] *p* AO's are constructed from two lobes each with offcenter shift d according to $d \cdot \sqrt{\eta} = 0.1$.
[b] c denotes the contraction coefficients, the groups are normalized to unity.

molecular centers of H_3^+ and H_2 and ϑ the angle between the H_2- and the intermolecular axis)

$$E_3 = R^{-3} Q_{H_2} P_2(\cos\vartheta) \tag{5}$$

and the monopole-induced dipole (H_2) term E_4

$$E_4 = -R^{-4}[\tfrac{1}{2}\alpha + \tfrac{1}{3}(\alpha_{||} - \alpha_\perp) P_2(\cos\vartheta)], \tag{6}$$

$$\alpha = \tfrac{1}{3}(2\alpha_\perp + \alpha_{||}). \tag{7}$$

Both types of interactions are approximately accounted for on the HF level. Within the present basis set we compute (on the HF level) the following values for Q_{H_2}, $\alpha_\perp$ and $\alpha_{||}$, exact values are given in parenthesis:

$$Q_{H_2} = 0.497 \text{ a.u.} \quad (0.460 \text{ a.u. [22] HF limit } 0.493 \text{ a.u. [23]}), \tag{8}$$

$$\alpha_{||} = 6.48 \text{ a.u.} \quad (6.381 \text{ a.u. [22]}), \tag{9}$$

$$\alpha_\perp = 4.48 \text{ a.u.} \quad (4.578 \text{ a.u. [22]}). \tag{10}$$

The close agreement between the present and the exact values clearly indicates that the HF approximation gives a reliable description of the long range $H_2 \cdot H_3^+$ interaction. We note that even rather small basis sets reproduce Q_{H_2} and $\alpha_{||}$ with satisfactory accuracy whereas it is necessary to include a rather smooth p function to reproduce $\alpha_\perp$ [13, 14].

The London dispersion interaction E_{disp}

$$E_{disp} = -R^{-6} C_6 (C_6 > 0) \tag{11}$$

(note that C_6 depends on the relative orientation of H_2 and H_3^+) is a genuine correlation effect and is not taken into account on the HF level. We note that E_{disp} coincides asyptotically (for large R) with the interpair correlation energy ε_{12}.

ε_{12} is of not too great importance as far as the gross features of the $H_2 \cdot H_3^+$ interaction is concerned since $|\varepsilon_{12}| < 0.07 \cdot \Delta E_{HF}$ for $R > 7$ a.u., but it cannot be neglected at the equilibrium configuration where ε_{12} amounts to 50% (C_{2v}) or 100% (D_{2h}, D_{2d}) of the corresponding HF binding energy ΔE_{HF}, compare section 5.

The computations with the present basis set are expected to give a reliable account of dispersion effects (E_{disp} and ε_{12}) since the latter are closely related to the polarizabilities of the interacting molecules which are accurately described by our basis. This fact was actually demonstrated for H_2 only, but the present author cannot see why this should be different for H_3^+.

At shorter intermolecular distances, where the charge clouds of H_2 and H_3^+ start to overlap, one further has the attractive forces of chemical binding, in the present case essentially a charge transfer from H_2 to H_3^+, repulsive forces due to the Pauli exclusion principle and the changes in intramolecular correlation $\Delta(\varepsilon_{11} + \varepsilon_{22})$.

Whereas the HF approximation accounts for the first two effects it clearly neglects $\Delta(\varepsilon_{11} + \varepsilon_{22})$.

With the present basis we get the following HF- and total energies for H_2 (d(H–H)=1.4 a.u.) and H_3^+ (equilateral triangle d(H–H)=1.66 a.u.), exact values in paranthesis:

$$E^{HF}(H_2) = -1.133005 \text{ a.u.} \quad (-1.1336)\,[24]$$
$$E^{PNOCI}(H_2) = -1.169609 \text{ a.u.} \quad (-1.17448)\,[24]$$
$$E^{HF}(H_3^+) = -1.298906 \text{ a.u.}$$
$$E^{PNOCI}(H_3^+) = -1.337931 \text{ a.u.}$$

Our HF- and total energies of H_2 differ by 0.0006 a.u. and 0.005 a.u. from the corresponding exact energies. The repective errors for H_3^+ are expected to be rather smaller than for H_2 since we have a larger total number of basis functions for the same number of electrons. We consequently estimate the absolute error of the computed electronic energies to about 0.01 a.u. (twice the error of H_2).

The deviation to the exact energies is essentially a "correlation effect" since we account for about 90% of the total correlation energy only. The remaining 10% are mainly due to the participation of d and f orbitals. These contributions may be expected to change only 1–2% of the total correlation energy only along any reaction path.

To sum up: The method of computation applied in the present study appears to give a reliable description of the most important intermolecule interactions between H_2 and H_3^+. The relative errors of the corresponding electronic energies are expected to be in the order of 10^{-3} a.u.

4. Gross Features of the $H_2 \cdot H_3^+$ Interaction

Previous studies indicate that H_5^+ forms a weakly bound ion cluster with only minor changes in the geometry of H_2 and H_3^+. For this reason we first performed a series of HF computations for various intermolecular distances and various relative orientations of H_2 and H_3^+ in their respective equlibrium geometry. The results are collected in Table 2 and Fig. 1. In these calculations we have thus not allowed for a relaxation of the H_2 and H_3^+ structures and have neglected correlation effects: $\varepsilon_{12}+\Delta(\varepsilon_{11}+\varepsilon_{22})$. These effects are of importance only for rather short intermolecular distances and cannot be neglected if we want to compute reaction energies with an accuracy of 1 kcal/mole. We therefore discuss the most interesting H_5^+ configurations in more detail in the next section. According to the discussion of the preceding section we expect however, that the HF approximation describes the gross features of the $H_2 \cdot H_3^+$ interaction.

Let us now discuss briefly the results collected in Table 2 and visualized in Fig. 1.

Cases 1–4: center of H_2 in H_3^+ plane, H_2 perpendicular to the intermolecular axis.

The four lowest lying curves are virtually indentical for $R>7$ a.u., where the interaction energies differ by less then 10%. This is not unexpected since the dominant long range interactions E_3 and E_4, compare Eqs. (5) and (6), (E_3 and E_4

Table 2. Hartree Fock interaction energies ΔE_{HF} for $H_2 \ldots H_3^+$ in 10^{-2} atomic units[a]

Geometry[a]		1	2	3	4	5	6	7	8
Location of H_2[b]		$(R, 0, \pm.7)$	$(R, \pm.7, 0)$	$(-R, 0, \pm.7)$	$(-R, \pm.7, 0)$	$(\pm.7, 0, R)$	$(R \pm .7, 0, 0)$	$(-R \pm .7, 0, 0)$	$(0, 0, R \pm .7)$
	20.0	−0.0045	−0.0045	−0.0045	−0.0045	−0.0030	0.0043	0.0043	0.0042
	15.0	−0.0120	−0.0119	−0.0119	−0.0118	−0.0071	0.0085	0.0074	0.0081
	10.0	−0.0499	−0.0493	−0.0488	−0.0478	−0.0236	0.0162	0.0159	0.0153
R	7.0	−0.1958	−0.1932	−0.1802	−0.1745	−0.0697	−0.0139	−0.0080	0.0031
a.u.	5.0	−0.6166	−0.6049	−0.4668	−0.4343	−0.0589	−0.0825	−0.0073	0.0967
	4.5	–	–	−0.4780	−0.4450[c]	–	–	–	–
	4.2	−0.7988	−0.7710	–	–	–	–	–	–
	4.0	−0.7706	−0.7464	−0.2575	−0.1446	0.6210	0.1403	0.767	1.0553
	3.0	1.3800	1.5183	2.6852	3.4650	4.6920	–	–	6.6204

[a] See also Fig. 1 and text. – [b] Nuclei of H_3^+ at positions $(0.9584, 0, 0)$ $(-0.4792, \pm 0.83, 0)$. – [c] $R = 4.8$.

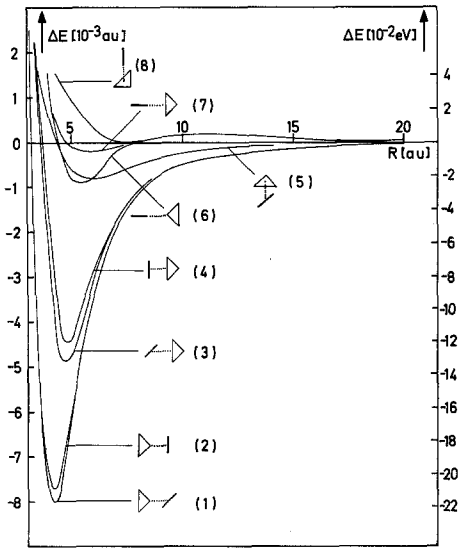

Fig. 1. Hartree Fock interaction energies ΔE_{HF} for $H_2 \ldots H_3^+$ (See also Table 2 and text)

are both attractive in this case since $\cos\vartheta = 0$ and $P_2(\cos\vartheta) = -1/2$), are identical for the respective geometries. D_e of curve 3 and 4 is only about 60% of that of curve 1 or 2. This is due to the fact that the electronic charge clouds in isolated H_2 and H_3^+ are slightly shifted from the nuclei into the bond regions. Consequently one expects stronger attractive forces (Coulomb interaction and charge transfer) and weaker repulsive forces (which arise from the overlap of charge clouds in connection with the exclusion principle) if H_2 approaches a corner of H_3^+, cases 1 and 2, than for the cases 3 and 4.

Case 5: H_3^+ plane and H_2 axis perpendicular to the intermolecular axis.

The long range interaction terms E_3 and E_4 for this geometry are identical to those of cases 1–4. We find, however, a markedly smaller interaction energy, even at $R = 20$ a.u. ΔE_{HF} is roughly 25% smaller than for the curves 1–4. This deviation indicates the importance of higher terms in the $1/R$-expansion, like quadrupole-quadrupole and monopole-hexadecapole interactions (both proportional to R^{-5}) at distances as large as 20 a.u. The short range forces of chemical binding are obviously very small in this case and we have a rather shallow potential curve.

Cases 6–8: H_2 in direction of the internuclear axis.

Different from geometries 1–5 we now have a repulsive monopole-quadrupole term E_3 since $\cos\vartheta = 1$ and $P_2(\cos\vartheta) = 1$. These curves are consequently repulsive for sufficiently large R where E_3 dominates the attractive induced dipole term E_4. The latter increases more rapidly if R decreases and the curves have a maximum at $R = 11.5$ a.u., and then a minimum at smaller R. A pronounced binding is found for case 6 only where H_2 approaches a corner of H_3^+, a position which is most favourable for a slight charge transfer and, hence, small chemical binding.

Barriers of Rotation

The differences of the D_e's of curve 1 and 2 (or 3 and 4, respectively) correspond to the barrier for a propeller-like rotation of H_2 around the intermolecular axis. This barrier is in both cases of the order of $3 \cdot 10^{-4}$ a.u. ($\approx 10^{-2}$ eV ≈ 100 °K). Due to the approximations made in the computations under consideration (neglect of correlation effects, no relaxation of structure parameters of H_2 and H_3^+), the actual values have possibly not too much significance but more refined computations confirm the order of magnitude.

The difference between the minima of curve 1 and 3 (or 2 and 4) correspond to the barrier of an in plane rotation of H_3^+. The corresponding barrier is about $3 \cdot 10^{-3}$ a.u. (≈ 0.08 eV ≈ 2 kcal/mol) and thus considerably smaller than the binding energy of H_5^+ (the curves 3 or 4, which correspond to the maxima of electronic energy along the H_3^+ rotation are quite strongly bound). This means that an H_5^+ collision complex has always sufficient internal energy for an in plane rotation of H_3^+.

5. The Effect of Relaxation and Electron Correlation on the Equilibrium Structure of H_5^+

5.1. More Accurate Determination of the Structure Parameters of H_5^+

We first varied the structure parameters for geometries 1 and 2 (C_{2v} symmetry) and also for the corresponding centrosymmetric D_{2d} and D_{2h} structures within the HF approximation. The H_2–H_3^+ distance for cases 1 and 2 and also the H_2–H_2 distance for the D_{2d} and D_{2h} structures were then reoptimized on the CEPA level. This procedure appeared necessary since the interpair correlation energy ε_{12} varies rapidly with the corresponding intermolecular distance. The final structures are described in Table 3.

The optimization procedure just described does not lead to drastic changes as compared to the results of the section 4. For structure 1 and 2 we find an increase of the H–H distance in the H_2 unit by roughly 0.01 a.u. The "central" proton of H_3^+ is shifted slightly towards the H_2 such that the H–H distances of the H_3^+ isosceles triangles are now 1.70 a.u. and 1.65 a.u. which may be compared to the H–H distance of 1.66 a.u. in free H_3^+. These changes in structure are consistent with a small charge transfer from H_2 to the "central" proton of H_3^+ and a shift of the H_3^+ electron pair into the basal H–H bond.

Table 3. Optimized structures for H_5^+ [a]

Structure	Position of		
	H1, H2	H3	H4, H5
$1(C_{2v})$ [b]	(−0.4955, ±0.825, 0)	(0.9907, 0, 0)	(3.94, 0, ±0.705)
$2(C_{2v})$ [b]	(−0.4955, ±0.825, 0)	(0.9907, 0, 0)	(3.99, 0, ±0.705)
D_{2d}	(±0.734, 0, −1.994)	(0, 0, 0)	(0, ±0.734, 1.994)
D_{2h}	(±0.7325, 0, −1.998)	(0, 0, 0)	(±0.7325, 0, 1.998)

[a] See text for a description of the structure determination.
[b] See also Table 2 and Fig. 1.

Table 4. Computed total energies for H_5^+ at optimized geometries[a]

Structure[a]	HF	PNO-CI	CEPA	ε_{H_2}[b]	$\varepsilon_{H_3^+}$[b]	ε_{12}[b]
$1(C_{2v})$	−2.44012	−2.51689	−2.51840	−0.03604	−0.03837	−0.00387
$2(C_{2v})$	−2.43987	−2.51648	−2.51797	−0.03532	−0.03774	−0.00354
D_{2d}	−2.43838	−2.51770	−2.51942	−0.03650	–	−0.00804
D_{2h}	−2.43783	−2.51701	−2.51872	−0.03644	–	−0.00801
$H_2 \ldots H_3^+$[c]	−1.43190	−2.50624	−2.50754	−0.03660	−0.03903	0.0

[a] See Table 3, all quantities in atomic units.

[b] ε_{H_2}, $\varepsilon_{H_3}^+$ denote the intrapair correlation energies of the H_2 and H_3^+ electron pair, ε_{12} the interpair correlation energy. The corresponding quantities are taken from the CEPA computation and add up to the CEPA correlation energy.

[c] H_2 and H_3^+ in their respective equilibrium geometry ($R_0(H_2) = 1.4$ a.u., $R_0(H_3^+) = 1.66$ a.u.) with intermolecular distance of 500 a.u.

As a result of the quite rapid increase of $|\varepsilon_{12}|$ with decreasing intermolecular distance R (measured with respect to the centers of gravity of the nuclei of H_3^+ and H_2) we find that R_0 decreases by about 0.2 a.u. if electron correlation is included.

The reoptimization of structure parameters for the cases 1 and 2 effects the total electronic energy by $0.5 \cdot 10^{-3}$ a.u. only (on the PNO-CI level) corresponding to roughly 5% of the binding energy.

As far as the D_{2d} and D_{2h} structures are concerned we note the increase of the H–H distance of the H_2 fragments to 1.47 a.u. as compared to 1.4 a.u. in H_2. This weakening of the H_2 bonds is a result of charge transfer to the central proton.

5.2. *Equilibrium Structure of* H_5^+

The total electronic energies obtained on the HF-, PNO-CI-, and CEPA level for the structures described in Table 3 are collected in Table 4. In this table we have also included a computation of $H_2 \ldots\ldots H_3^+$ at large intermolecular distance $R = 500$ a.u. This calculation is necessary as a reference point to determine D_e on the PNO-CI level. The PNO-CI (like any CI with double substitutions only) does not converge (for large R) towards the sum of the PNO-CI energies of the corresponding subsystems even if the latter are closed shell systems [18]. In order to determine D_e on the PNO-CI level we consequently compare the PNO-CI energies of H_5^+ with that of the system $H_2 \ldots\ldots H_3^+$.

We first note that structure 1 still corresponds to the minimum of the HF potential hypersurface. The HF energies of case 2, the D_{2d} and D_{2h} structures are $0.25 \cdot 10^{-3}$, $1.73 \cdot 10^{-3}$, and $2.3 \cdot 10^{-3}$ a.u. higher than for structure 1.

The computed total energies on the PNO-CI and CEPA level predict the D_{2d} structure to be lowest in energy. The corresponding total energies for structure 1, however, are only 10^{-3} a.u. higher. Such a small energy defference is just at the limit of accuracy of the present computations. Since most of the structure parameters collected in Table 3 were determined on the HF level, we wondered whether case 1 corresponds at least to a local minimum and if the D_{2d} structure is the absolute minimum. Additional computations proved, in fact, that structure 1 is not even a local minimum (on the PNO-CI- and CEPA level) and that the

potential surface near the D_{2d} structure is extremely shallow. Structures half way in between case 1 and D_{2d} still have energies which differ by less than 10^{-4} a.u. from that of the D_{2d} geometry. Energy differences of this order of magnitude are beyond the accuracy of the present study and our investigations essentially prove that the equilibrium structure of H_5^+ is D_{2d} (or rather close to D_{2d}) with an extremely great mobility of the central proton.

Inclusion of electron correlation changes in the case of H_5^+ the order of the computed energies for the structures considered. This is mainly due to the effect of interpair correlations ε_{12}. In the D_{2d} and D_{2h} structure one finds a larger differential overlap of the localized MO's than in case 1 or 2. This results in a significantly larger ε_{12} of $0.80 \cdot 10^{-2}$ a.u. (D_{2d}) as compared to $0.39 \cdot 10^{-2}$ a.u. (structure 1).

5.3. Enthalpy of Formation of H_5^+

Using the minima of the respective HF-, PNO-CI-, and CEPA potential surface of H_5^+ we first obtain the following D_e for reaction (1)

$$\text{HF:} \quad D_e = 5.1 \text{ kcal/mol} \tag{12}$$

$$\text{PNO-CI:} \quad D_e = 7.2 \text{ kcal/mol} \tag{13}$$

$$\text{CEPA:} \quad D_e = 7.4 \text{ kcal/mol}. \tag{14}$$

Our HF result is in rather good agreement with the best previous HF computation by Huang, Schwarz and Pfeiffer [11], who obtained $D_e = 4.25$ kcal/mol. The HF energy obtained by these authors for H_5^+ ($E_{HF} = -2.43776$ a.u.) is about 1 kcal/mol higher than the present result. This deviation is due to the fact that the present basis is more flexible (than the one used in Ref. [11]) and contains smoother s and p functions which are necessary to obtain an accurate description of binding energies for weakly bound systems with rather large interatomic distances. For the same reason we get for the D_{2d} structure on the HF level $D_e = 4.1$ kcal/mole, whereas the most extended previous study [12] predicted $D_e = 0.6$ kcal/mole for this case. The discrepancy between our most reliable D_e, Eq. (14), and the result of Salmon and Poshusta [12], $D_e = 3.9$ kcal/mole, may also be attributed to the rather limited basis used by these authors.

In order to obtain ΔH^0 one has to evaluate the following terms (in an obvious notation)

$$\Delta H^0(T) = -D_e + \Delta E_v(T) + \Delta(E_{rot}(T) + E_{kin}(T) + pV). \tag{15}$$

At 300 °K we can treat the last term on the r.h.s. of (15) classically and obtain at $T = 300$ °K,

$$\Delta(E_{rot} + E_{kin} + pV) = -2.1 \text{ kcal/mole}. \tag{16}$$

To obtain an estimate of $\Delta E_v(T)$ proved to be extremely difficult. The effect of zero point vibrations has been estimated by Salmon and Poshusta [12] to 250 cm^{-1}. These authors assumed, however, that the vibration frequencies of the

H_2 and H_3^+ fragments in H_5^+ are the same as in the free molecules. This assumption appears to be oversimplified since the present work proves the great mobility of the central proton.

We have tried to determine the normal modes for the D_{2d} geometry in the harmonic approximation. This attempt proved to be rather useless, however, since one of the B_2 modes (which corresponds to the displacement of the central proton along the molecular axis) has a harmonic frequency $\omega_0 < 150\,\mathrm{cm}^{-1}$ (by virtue of the above discussions this result is not unexpected, of course). This corresponds to a mean square displacement $q^2 > (1a_0)^2$. As the remaining force constants change too much along this vibration we cannot apply the harmonic approximation to describe the nuclear motions.

In order to obtain at least a rough estimate for ΔH^0 we therefore simply assumed that the zero point vibrations have no effect on ΔH^0 and that the B_2 mode discussed above contributes roughly RT. If we further assume that the propeller-like rotation, B_1 in D_{2d} symmetry, may be considered as a free rotation $\left(\text{which contributes } \frac{R}{2}T \text{ to the enthalpy}\right)$ and that all other vibrations of H_5^+ and also those at H_2 and H_3^+ are not thermally excited at 300 °K, we obtain

$$\Delta E_v(300\,^\circ\mathrm{K}) = 0.9\ \mathrm{kcal/mole}$$

and further with Eq. (14–16)

$$\Delta H^0 = -8.7\ \mathrm{kcal/mole}\,. \tag{17}$$

Equation (17) should rather be considered as a rough guess, since we were not able to treat vibrations in a thorough way. This would require to compute the H_5^+ surface for a rather wide range of atomic displacements to a high accuracy and then to solve the vibrational Schrödinger equations. Due to the excessive amount of computertime needed for such computations it was considered to be beyond the scope of this study. The present result, however, is in good agreement with the recent experimental value of Bennett and Field [7].

6. Concluding Remarks

The present study appears to be the first theoretical treatment of H_5^+ which can claim "chemical accuracy", i.e. an error of 1–2 kcal/mole for the computed energy differences. Our results differ in some respects from those of previous studies [8–12] which is due to the fact that we used a more extended basis set and a more refined method of computation than employed previously. As far as the HF approximation is concerned we confirm previous conclusions [11] that a non-planar ion cluster $H_2 \cdot H_3^+$ with C_{2v} symmetry corresponds to the minimum of the HF potential surface. Electron correlation, however, has not only a marked influence on D_e, compare Eqs. (12) and (14), it also brings the energy of the D_{2d} structure below that of the ion cluster $H_2 \cdot H_3^+$. The potential surface is extremely shallow in the neighbourhood of the D_{2d} structure and the vibration of the central proton along the molecular axis (corresponding to a displacement in direction of

the $H_2 \cdot H_3^+$ structure) is highly excited at room temperature. One can consequently say that H_5^+ spends actually most of the time in the $H_2 \cdot H_3^+$ structure (at $T = 300\,°K$).

Let us finally point out that the present results offer the following explanation for the relatively large cross section for the reactive scattering process (3) at low scattering energies:

$H_3^+ + D_2 \rightarrow H_2 + HD_2^+$ (transfer of the "central nucleus")

$\rightarrow H_2 + DHD^+$ (in plane rotation of HD_2^+) $\rightarrow H_2D^+ + HD$ (transfer of the "central nucleus").

We have already pointed out in section 4 that the H_5^+ collision complex has sufficient internal energy for all steps of such a process, which should occur if the collision time is comparable to the time for an in plane rotation of H_3^+.

Acknowledgements. The author is indebted to Prof. Ch. Schlier and Dr. E. Teloy, Universität Freiburg, and to Prof. W. Kutzelnigg, Universität Bochum, for numerous valuable discussions. Part of the computations were performed with the assistence of Miss Baud. The computertime was made available by the „Rechenzentrum der Universität Karlsruhe". This work was supported by the „Deutsche Forschungsgemeinschaft" and, in part, by the „Fonds der Chemischen Industrie".

References

1. Dawson, P.H., Tickner, A.W.: J. Chem. Phys. **37**, 672 (1962)
2. Kirchner, F.: Z. Naturforsch. **A18**, 879 (1963)
3. Saporoschenko, M.: J. Chem. Phys. **42**, 2760 (1965); Phys. Rev. **139**, A 349 (1965)
4. Buchheit, K., Henkes, W.: Z. Angew. Phys. **24**, 191 (1968)
5. Clampitt, R., Gowland, L.: Nature (Lond.) **223**, 815 (1969)
6. Arifov, U.A., Pozharov, S.L., Chernov, I.G., Mukhamediev, Z.A.: Khim. Vys. Energ. **1971**, 5 (1) 81 (High Energy Chem. **5**, 69 (1971))
7. Bennett, S.L., Field, F.H.: J. Am. Chem. Soc. **94**, 8669 (1972)
8. Poshusta, R.D., Matsen, F.A.: J. Chem. Phys. **47**, 4795 (1967)
9. Poshusta, R.D., Haugen, J.A., Zetik, D.F.: J. Chem. Phys. **51**, 3343 (1969)
10. Easterfield, J., Linnett, J.W.: Chem. Commun. **1970**, 64
11. Huang, J.-T.J., Schwartz, M.E., Pfeiffer, G.V.: J. Chem. Phys. **56**, 755 (1972)
12. Salmon, W.I., Poshusta, R.D.: J. Chem. Phys. **59**, 4867 (1973)
13. Kochanski, E.: Chem. Phys. Letters **15**, 254 (1972)
14. Jungen, M., Ahlrichs, R.: Mol. Phys. **28**, 367 (1974)
15. private communication of E. Teloy and Ch. Schlier, Freiburg
16. Edmiston, C., Krauss, M.: J. Chem. Phys. **42**, 1119 (1965), **45**, 1833 (1966)
17. Ahlrichs, R., Driessler, F.: Theoret. Chim. Acta (Berl.), **36**, 275 (1975)
18. Ahlrichs, R., Lischka, H., Staemmler, V., Kutzelnigg, W.: J. Chem. Phys. **62**, 1225 (1975)
19. Meyer, W.: Intern. J. Quantum Chem. S **5**, 341 (1971), J. Chem. Phys. **58**, 1017 (1973)
20. Ahlrichs, R.: Theoret. Chim. Acta (Berl.) **35**, 59 (1974)
21. Keil, F., Ahlrichs, R.: submitted for publication
22. Kolos, W., Wolniewicz, L.: J. Chem. Phys. **46**, 1426 (1967)
23. McLean, A.D., Yoshimine, M.: J. Chem. Phys. **45**, 3676 (1966)
24. Kolos, W., Wolniewicz, L.: J. Chem. Phys. **43**, 2429 (1965)

Dr. R. Ahlrichs
Institut für Physikalische Chemie
und Elektrochemie der Universität Karlsruhe
D-7500 Karlsruhe, Postfach 6380
Federal Republic of Germany